Role of Future Reef Growth on Morphological Response of Coral Reef Islands to Sea-Level Rise

G. Masselink[1], R. McCall[2], E. Beetham[3], P. Kench[4], C. Storlazzi[5]

[1]Coastal Processes Research Group, School of Biological Sciences, University of Plymouth, Plymouth, PL4 8AA, United Kingdom. [2]Deltares, Delft, 2629 HV, the Netherlands. [3]Tonkin and Taylor International Ltd, Auckland 1023, New Zealand. [4]Department of Earth Sciences, Simon Fraser University. BC V5A 1S6, Canada. [5] Pacific Coastal and Marine Science Center, USGS, Santa Cruz, CA 95060, USA.

Corresponding author: Gerd Masselink (g.masselink@plymouth.ac.uk)

Key Points

- A process-based numerical model can be used to model the response of gravel and sand coral reef islands to sea-level rise (SLR)
- Reef islands evolve during SLR by attuning their elevation to the maximum wave runup; therefore, gravel islands build up higher than sand islands
- As long as mean overwash discharge across the island crest is below a certain threshold $O(10\ \mathrm{l\,m^{-1}\,s^{-1}})$ coral reef islands accrete vertically during sea-level rise
- Future reef growth does not increase the ability of islands to adjust to sea-level rise on the medium-term (< 50 years)

Abstract

Coral reefs are widely recognised for providing a natural breakwater effect that modulates erosion and flooding hazards on low-lying sedimentary reef islands. Increased water depth across reef platforms due sea-level rise (SLR) can compromise this breakwater effect and enhance island exposure to these hazards, but reef accretion in response to SLR may positively contribute to island resilience. Morphodynamic studies suggest that reef islands can adjust to SLR by maintaining freeboard through overwash deposition and island accretion, but the impact of different future reef accretion trajectories on the morphological response of islands remain unknown. Here we show, using a process-based morphodynamic model, that, although reef growth significantly affects wave transformation processes and island morphology, it does not lead to decreased coastal flooding and island inundation. According to the model, reef islands evolve during SLR by attuning their elevation to the maximum wave runup and islands fronted by a growing reef platform attain lower elevations than those without reef growth, but have similar overwash regimes. The mean overwash discharge Q_{over} across the island crest plays a key role in the ability of islands to keep up with SLR and maintain freeboard, with a Q_{over} value of $O(10\ \mathrm{l\,m^{-1}\,s^{-1}})$ separating island construction from destruction. Islands, therefore, can grow vertically to keep up with SLR via flooding and overwash if specific forcing and sediment supply conditions are met, offering hope for uninhabited and sparely populated islands. However, this physical island response will negatively impact infrastructure and assets on developed islands.

Plain Language Summary

Coral reef islands are low-lying (generally less than 4 m above mean sea level) and are particularly exposed to the impacts of sea-level rise. These islands are usually fronted by ‘living’coral reef platforms that protect the island shoreline from energetic wave action by acting like a breakwater. Healthy reef platforms grow vertically and can potentially keep up with rising sea level, maintaining a constant water depth in front of the island. It is therefore suggested that future reef growth may be a critical factor in reducing the vulnerability of coral reef islands to sea-level rise. To investigate this suggestion, we use a computer model to simulate the response of coral reef islands to sea-level rise with and without future reef growth. We find that as sea level rises, the islands evolve by retreating, while at the same time building up vertically. Island build up is accomplished by waves overwashing the island and depositing sediment on the top and back of the island. The maximum elevation of the evolving island is controlled by how high the waves run up the beach. According to our model results, vulnerability of the reef islands to sea-level rise is not dependent on whether the reef platform grows or not. In both cases, islands are regularly flooded and overwashed, but these processes are necessary for islands to grow vertically. Island accretion by overwash offers hope for uninhabited and sparely populated islands but will negatively impact infrastructure and assets on urbanized islands.

1 Introduction

Coral reef islands are wave-built accumulations of carbonate sediment deposited on sub-horizontal reef platforms with a reef edge that slopes steeply to deeper water. A characteristic feature of these islands is their low-lying nature (< 4 m above mean sea level), which makes them susceptible to coastal flooding and island inundation during extreme events, such as cyclones (Scoffin, 1993), long-period wave events (Wadey et al., 2017) and tsunamis (Kench et al., 2006). Of particular concern to the communities living on these islands is the increased probability of wave-driven flooding due to future sea-level rise (SLR) and possibly increased storminess, and it is widely assumed that the islands will become increasingly uninhabitable through this century (Storlazzi et al., 2018), threatening the very existence of the coral reef island nations (Magnan and Duvat, 2018). However, these pessimistic outlooks are based on both the reef platform and the island being geologically inert structures, and disregard two important processes that may positively contribute to island resilience to SLR.

Firstly, coral reefs are sea-level limited and future SLR will open accommodation space for vertical reef accretion (Perry et al., 2012; Woodroffe and Webster, 2014), providing a self-regulating mechanism to mitigate the physical impacts of SLR on reef islands. Reef growth is likely to be compromised in many reef regions as a consequence of a global decline in coral cover, increased sea surface temperatures, ocean acidification and anthropogenic stresses (Hoegh-Guldberg, 1999; Pandolfi et al., 2011; van Woesik et al., 2015; Hughes et al., 2017). However, recent studies have documented coral re-colonization across previously emergent low-enery reef flats in pristine areas due to SLR (Brown et al., 2011; Scopélitis et al., 2011) and land subsidence (Saunders et al., 2016), providing evidence that locally some reefs may have capacity to vertically accrete and keep pace with future sea-levels. The potential for vertical reef growth to keep pace with SLR is therefore likely to be spatially variable and contingent on the existing health of coral reefs (Perry et al., 2018; Ryan et al., 2019; van Woesik and Cacciapaglia, 2018, 2019).

Secondly, similar to all coastal morphodynamic systems (e.g., salt marhes, mangroves, barrier systems), coral reef islands can respond or adjust morphologically to SLR through sediment transport. Recent physical (Tuck et al., 2019a, b) and numerical (Masselink et al., 2020) modelling has demonstrated that overwash processes, the frequency of which will be enhanced by SLR, can result in island accretion and raising of the crest level, as well as island retreat. Such conclusions are supported by field evidence documenting washover deposition on island surfaces in response to a range of wave driven mechanisms (Kench et al. 2006; Hoeke et al., 2013; Kench and Beetham, 2019). This 'roll-over' response is well documented in gravel barrier studies (Orford et al., 1995) and is characterised by the migration of the barrier (or island) through erosion of the ocean shoreline and deposition at the back of the barrier (or island) and/or the the lagoon shoreline. The response of reef islands to SLR depends on a range of forcing factors, such as rate of SLR and changes in the storm wave climate, and controlling factors, such as sediment supply, island geometry and reef platform topography, but reef islands are potentially able to maintain freeboard (difference between island crest level z_{crest} and still water level SWL) through overwash-induced vertical island accretion (Masselink et al., 2020).

Reef platforms that surround islands are generally considered to play a key role in protecting islands from erosion and flooding as they dissipate incident ocean wave energy and control residual energy reaching the shoreline (Ferrario, 2014; Cheriton et al., 2016). Increased sea levels will fundamentally change this protective role and modify the receipt of wave energy at shorelines, potentially exposing islands to increased shoreline erosion and island flooding (Quataert et al., 2015; Beetham et al., 2017; Beetham and Kench, 2018). Critical factors governing the energy incident at island shorelines are the still water depth across the platform h_{reef} and the width of the platform w_{reef}, and both have been explored using the BEWARE data set (Pearson et al., 2017) that was generated with the non-hydrostatic version of the process-based XBeach model (Smit et al., 2011; McCall et al., 2014) by exposing a set of idealized reef platforms and island configurations to a wide range of forcing conditions to investigate wave runup and wave-induced flooding (Figure **S1**). These model data demonstrate that the incident wave height at the toe of the beach and the wave runup, and thus the risk of wave-induced flooding, increases with water depth across the platform (cf., Quataert et al., 2015; Beetham et al., 2017; Pearson et al., 2017), while the infragravity wave height at the toe of the beach and the wave setup increases with decreased water depth across the platform (cf., Masselink et al., 2018).

It can thus be surmised that if the reef platform vertically accretes at the same rate as SLR (h_{reef} = constant), the protective role of the platform will be maintained, but if the platform surface does not keep up (h_{reef} increases), greater water depths across the platform will expose the reef island to increasingly energetic conditions (Quataert et

al., 2015; Cheriton et al., 2016; Beetham et al., 2017). However, the reef platform is not the only feature that may evolve during SLR, as the reef island may also adjust (Tuck et al., 2019a, 2019b). The aim of this paper is therefore to explore the role of reef platform growth on the ability of coral reef islands to morphodynamically adjust to SLR under energetic wave conditions (H_0 = 3 m). We follow a similar modelling approach as that followed by Masselink et al. (2020), but extend the analysis by considering the response of both gravel and sand islands, accounting for reef growth and modelling SLR of up to 2.5 m, and also considering the impact moderate (H_0 = 2 m) to extreme (H_0 = 5 m) wave conditions.

2 Materials and Methods

The XBeach-G (McCall et al., 2014, 2015) numerical model, which is the 1DH, phase-resolving, gravel version of the XBeach model (Roelvink et al., 2009) that accounts for groundwater interactions, was used in this study. Sediment transport was computed using Nielsen (2002) with a phase angle of 30°, a wave friction factor of 0.01 and accounting for the local slope (for more information, refer to Masselink et al., 2020). An initial XBeach model was set up (Figure **1a**), characterized by an immovable and impermeable reef platform (w = 700 m; z = 0 m), with steep ($\tan\beta$ = 0.5) reef slopes on both sides that terminate in a horizontal surface (z = -25 m). A permeable and movable island was placed on the platform with a width w of 300 m and 200 m at the base and top, respectively, and a crest height z_{crest} of 5 m and 4 m at the exposed ocean and lagoon shorelines, respectively. The associated ocean beachface, island-top and lagoon beachface slopes were 0.100, 0.005 and 0.080, respectively. The model grid size of the horizontal reef platform and island section was 0.25 m, and increased for the sloping reef edge and deep-water section from 0.25 m at z = 0 m to 3.25 m at z = -25 m. The island was composed of either gravel and sand material, and the associated median sediment size D_{50} and hydraulic conductivity K were 0.014 m and 0.001 mm, and 0.005 m s^{-1} and 0 m s^{-1}, respectively. The sand island was made impermeable to maximize the constrast with the gravel island to help bring out disparate behavour. All models were forced with 1-hr segments of wave forcing defined by a JONSWAP spectrum with a gamma value of 3.3, and with instantaneous morphodynamic updating (XBeach model parameter '*morfac* = 1'). For all morphodynamic simulations (Sections 2, 3.1, 3.2, 3.4 and 3.5), hourly wave forcing varied stochastically ('*instat* = *jons*'), whereas for the hydrodynamic simulations (Sections 3.3) an identical wave forcing signal was used ('*instat* = *reuse*'). All simulations were done for gravel and sand, and an overview of all model runs is provided in Table **1**.

Table **1** – Key XBeach model settings: H_0 = offshore significiant wave height; T_p = peak wave period; *instat* = XBeach setting referring to stochastic wave signal (*jons*) or previously used (*reuse*) wave signal; *Sea level* = water level relevative to reef platform elevation at start of simulation; *Duration* = individual run length; *Morph. updating* = whether morphology is being updated during model run; *Reef growth* = whether the reef platform elevation keeps pace with SLR; *Initial morph.* = morphology at start of simulation. All simulations were done for gravel and sand.

Test	***H_0* (m)**	***T_p* (s)**	***instat***	***Sea level* (m)**	***Duration* (hr)**	***Morph. updating***	***Reef growth***	***Initial morph.***	**Purpose**
A	1–6	9.9	jons	2	3	yes	no	idealised	Identify appropriate wave condition
B	3	9.9	jons	2	250	yes	no	Idealized	Investigate equilibrium
C	3	9.9	jons	2 → 3	50, 100, 200	yes	no	Primed	Role of rate of SLR
D	3	9.9	jons	2 → 4.5	250	yes/no	yes/no	Primed	Role of reef growth
E	3	9.9	reuse	2 → 4.5	3	no	no	Test D at t = 0,10,20,…	Hydrodynamics during Test D
F	1–5	9.9	jons	4.5	1	yes	no	Test D at t = 200	Role of wave height variability
G	2–5	9.9	jons	2 → 4.5	250	yes	yes	Primed	Role of wave height variability

The platform-island topography used for the numerical modelling is considered characteristic of many atoll rim islands (e.g., Woodroffe, 2008; Kench et al., 2017). To select the default wave and tide level conditions for the model simulations it was assumed that incremental island adjustment is primarily accomplished during conditions that just reach the island crest; moderate conditions only shape the island beach (Kench et al., 2009, 2017) and extreme conditions result in large-scale transformation of the island structure. It is also assumed that conditions that

significantly modify the top of the island are limited to high tide and/or extreme events when setup levels across the reef flat and shoreline are elevated, and this was considered to be at z = 2 m (resulting in a still water depth across the reef platform h_{reef} of 2 m). A characteristic peak wave period T_p of 9.9 s was used. A large number of 3-hr test simulations were conducted with offshore significant wave heights inreasing from H_0 = 1 m to 6 m in 0.5-m steps (**Test A**; Table **1**). It was found that for H_0 < 2.5 m, wave runup did not reach the island crest and that for H_0 > 3.5 m, a large amount of overwashing occurred, significantly modifying both the gravel and sand island, and causing considerable crest accretion for the gravel island and crest retreat for the sand island (Figure **1b-e**). The associated across-reef variation in significant wave height H_s is displayed in Figure **1a** and shows wave breaking at the reef edge followed by wave dissipation and wave setup across the reef platform. A value of H_0 = 3 m was used for simulations B–E as it represents the wave forcing that would lead the the development of the crest at a level approximately equal to that of the initial island profile. Selection of such a 'formative' wave condition is analogous to the concept of a bankful discharge in hydrology, where river channel characteristics (width, depth, cross-section) are related to the flow that reaches the transition between the channel and adjacent flood plain.

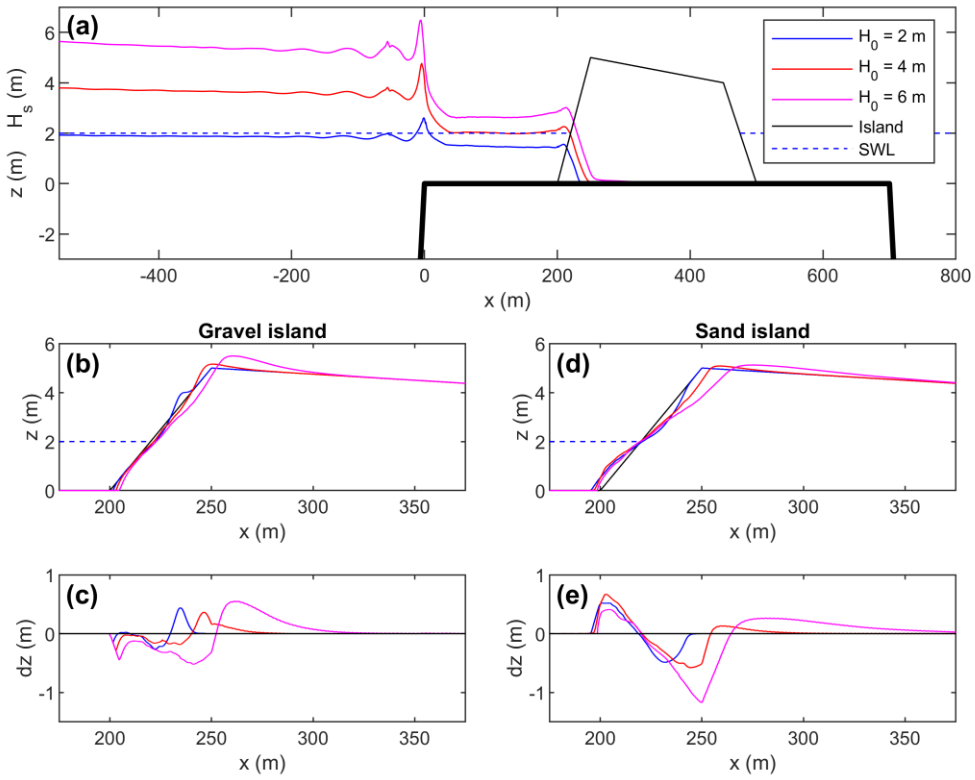

Figure **1** – XBeach model results for varying wave forcing: (a) cross-shore variation in H_0 and general reef-island set-up; (b) and (c) profile evolution for different wave forcing for gravel island (D_{50} = 14 mm, K = 0.005 m s^{-1}); (d) and (e) profile evolution for different wave forcing for sand island (D_{50} = 1 mm, K = 0 m s^{-1}). H_0 = 2–6 m, T_p = 9.9 s, h_{reef} = 2 m and each model run lasted 3 hrs. [p_test_series_0_V2]

Although the elevation of the island broadly corresponds to the maximum runup associated with H_0 = 3 m, T_p = 9.9 s, h_{reef} = 2 m and tanβ = 0.1, the morphology of the front of the idealized island (i.e., the 'beachface') is unlikely to reflect the exact shape and position that is in equilibrium with those forcing conditions. To avoid 'contaminating' the morphological response of the island to SLR by the morphological adjustments towards an equilibrium profile shape, the island morphology was 'primed' before starting any sea-level simulations and the 'primed' island morphology was used as a starting point for the sea-level simulations (**Test B**; Table **1**). Figure **2b,c** shows the gravel and sand island morphology after 250 hrs of constant wave and water-level conditions (H_0 = 3 m, T_p = 9.9 s, h_{reef} = 2 m), and Figure **2d,e,f** shows time series of some key morphometric parameters: cumulative gross morphological change $|Q_{sed}|$, island crest elevation z_{crest} and island crest position x_{crest}. Figure **2a** shows the associated wave and set-up profile across the reef platform.

The gravel island response to the 'priming' period is characterised by onshore sediment transport, resulting in a steepening of the beachface from $\tan\beta = 0.1$ to 0.15 and the construction of a small berm (0.8 m high) at the original island crest position. Sediment transport on the sand island is offshore across the submerged part of the beachface and onshore in the swash zone, resulting in a flattening of the beachface from $\tan\beta = 0.1$ to 0.05, the construction of a small submerged bar and subaerial berm (0.9 m and 0.2 m high, respectively), and 15 m retreat of the island crest. The gravel island response involves less cumulative gross change than on the sand island ($|Q_{sed}|$ = 100 m^3 m^{-1} and 200 m^3 m^{-1}, respectively), but for both islands 75% of the total $|Q_{sed}|$ over the 250-hr model simulations is accomplished during the first 50 hrs (Figure **2d**), suggesting that equilibrium is being approached. This is also indicated by the overwash discharge Q_{over} at the crest location, which, on both types of islands, progressively decreases during the simulation from 0.5 l m^{-1} s^{-1} to insignificant (Figure **2g**). Note that no further change can occur at the island crest if the overwash discharge approaches zero. The gravel and sand island morphology after 50 hrs of modelling is used as the 'primed' profile for all sea-level simulations. It is acknowledged that this does not represent a 'true' equilibrium – both islands will keep incrementally increasing their crest elevation as long as the steepening beachface results in increased wave runup elevation – but the rate of change after 50 hrs of constant sea level is an order of magnitude less than the morphological change that occurs in response to SLR.

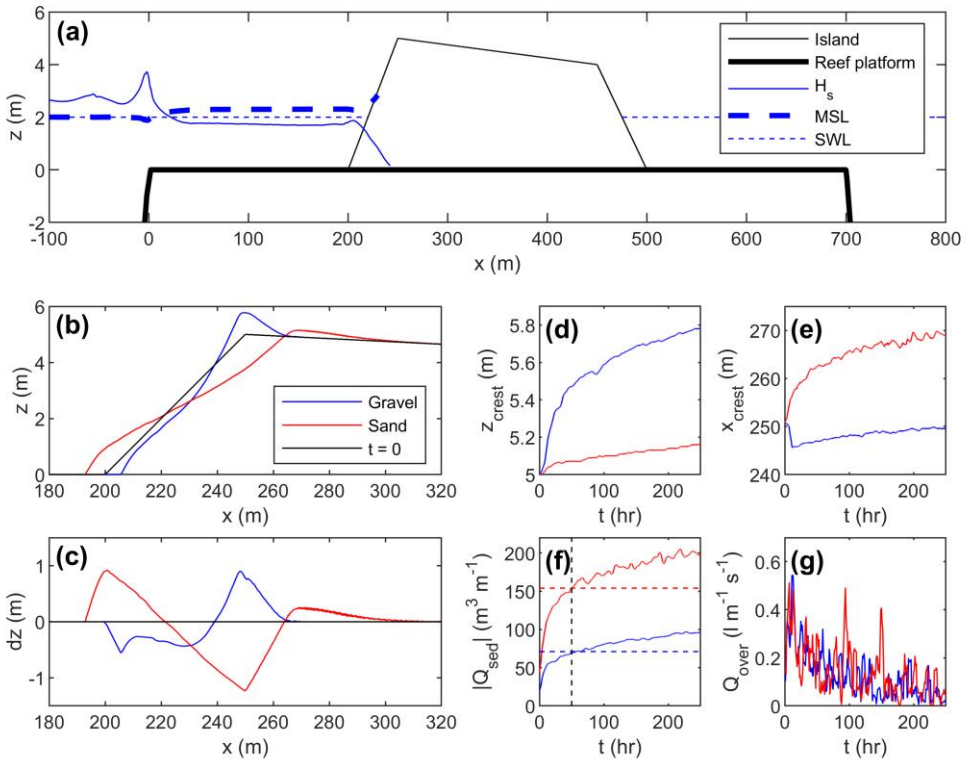

Figure **2** – XBeach-G model results for 250-hr simulation with constant wave forcing of H_0 = 3 m, T_p = 9.9 s and h_{reef} = 2 m, for gravel (D_{50} = 14 mm, K = 0.005 m s^{-1}) and sand (D_{50} = 1 mm, K = 0 m s^{-1}) island. (a) Model set-up with cross-shore variation in significant wave height H_s, wave set-up MSL and the tide level SWL. (b) Island morphology z and (c) morphological change dz after 250-hr of wave action. Time series of (d) island crest elevation z_{crest}, (e) island crest position x_{crest}, (f) cumulative gross morphological change $|Q_{sed}|$ and (g) overwash discharge Q_{over} across the island crest. The horizontal dashed lines in (d) represents 75% of the total $|Q_{sed}|$ over the 250-hr simulation, which occurred for both the gravel and sand simulation around t = 50 hrs (vertical dashed line). The time series were smoothed using a 5-hour moving window. [p_equilibrium_axes]

Using a processed-based model operating in real-time, such as XBeach-G, to model long-term coastal evolution as a result of SLR is potentially problematic and, at least, challenging. An 'input-filtering' approach was used here that assumes that whole-island change is only accomplished by extreme and infrequent wave conditions acting at high

tide (cf., Masselink et al., 2020). Specifically, the rate of SLR was linked to hours of extreme wave action (H_0 = 3 m) operating at high tide (h_{reef} = 2 m at the start of the simulation). The island response to 1-m SLR was explored for three variations in total duration of extreme wave action occurring during the SLR period: 50, 100 and 200 hr, representing 0.02 m hr^{-1}, 0.01 m hr^{-1} and 0.005 m hr^{-1} rate of SLR per hour of extreme wave conditions, respectively (**Test C**; Table **1**). Assuming such conditions occur one hour per year on average, the three rates represent annual SLR rates of 0.02 m yr^{-1}, 0.01 m yr^{-1}, and 0.005 m yr^{-1}, respectively (i.e., 1-m SLR occurring in 50, 100, or 200 yr, respectively). Alternatively, the three rates represent a variation in the number of hours of extreme waves per year for a given annual SLR rate, e.g., 0.5, 1 and 2 hr of extreme waves per year for a constant annual SLR rate of 0.01 m yr^{-1}. As such, the approach is decoupled from SLR rate projections and instead describes the relationship between the speed at which sea level is rising and the available time to build up the island crest in response. This event-based modelling approach does not fully describe coral reef island evolution over long time scales; however, the approach offers an experimental platform with which to consider the role of a range of important factors in coral reef island response to SLR, including sediment size, reef platform growth and wave height variability.

After the 1-m SLR simulations, the response of gravel and sand islands to 2.5 m of SLR at a rate of 0.01 m hr^{-1} of extreme waves was simulated with and without reef growth (**Test D**; Table **1**). For the model simulations with reef growth, the reef accretes at the same rate as SLR, but lagged behind by 1 hr (i.e., 0.01 m). When first accounting for reef growth, only that part of the reef platform not covered by sediment was allowed to grow, but island retreat due to roll-over resulted in the development of an unrealistically deep (> 1 m) 'moat' in front of the retreating island. In reality, such moat would be filled with sediment, but this does not happen according to the model. Instead, therefore, in the subsequent simulations with reef growth, the entire reef platform was allowed to grow with SLR, even underneath the island, but without modifying the elevation of the island. This approach does this effectively lock up island sediment below the level of the reef platform and limits the amount of sediment available for remobilisation and reworking during island retreat.

To investigate in detail the hydrodynamic conditions during the reef growth simulations, hourly-averaged hydrodynamics were output for every 10th hour of the 2.5-m SLR simulations (i.e., t = 0, 10, 20, 30, … hrs, or SLR = 0, 0.1, 0.2, 0.3, … m). For these model runs (**Test E**; Table **1**), exactly the same hourly wave forcing was used throughout (H_0 = 3 m, T_p = 9.9 s), but four different morphological boundary conditions were used: (1) unmodified 'primed' island morphology; (2) unmodified 'primed' island morphology with a raised reef platform; (3) modelled island morphology with static reef platform; and (4) modelled island morphology with reef platform growth.

To start exploring the role of wave height variability on island response, the gravel and sand island morphology attained after 200 hrs of SLR with reef growth was exposed to a large number of 1-hr simulations with H_0 increasing from 1 m to 5 m in 0.1-m steps and a sea level at 2.5 m, i.e., 0.5 m higher than corresponding to t = 200 hrs (**Test F**; Table **1**).

In the final set of simulations, island response to a 2.5-m SLR at a rate of 0.01 m hr^{-1}, and accounting for reef growth, was modelled, but this time with variable wave conditions (**Test G**; Table **1**). Forcing wave conditions were randomly selected from a triangular H_0 distribution with maximum probability for H_0 = 2 m and zero probability for H_0 = 5 m. The resulting 250-hr time series of H_0 was characterised by a rms value of 3.1 m, thus representing only a slightly higher wave energy level than during the previous simulations with a constant wave height of H_0 = 3 m.

3 Results

3.1 Role of rate of sea-level rise on island response

The modelled evolution of the gravel and sand reef island in response to a 1-m increase in sea level from +2.0 to +3.0 m for the three different rates of SLR (**Test C**; Table **1**) is shown in Figure **3**. During all simulations, the island demonstrates roll-over behavior (Figure **3a,f**), but the gravel island accretes and retreats more (Δz_{crest} = 0.4–0.7 m; Δx_{crest} = 7–10 m; Figure **3b,c**) than the sand island (Δz_{crest} = 0.1–0.3 m; Δx_{crest} = 5–7 m; Figure **3g,h**). The cumulative onshore sediment transport Q_{sed} across the island crest is also larger for the gravel island (Q_{sed} = 7–11 m^3 m^{-1}; Figure **3d**) than the sand island (Q_{sed} = 3–9 m^3 m^{-1}; Figure **3i**). The island crest accretes in all simulations, but the amount of freeboard (z_{crest}-SWL, where SWL denotes still water level) reduces throughout the simulation, especially for the sand island and for the fastest rate of SLR. This reduction in freeboard results in increased overwash discharge across the island crest during the simulations, but less so for the gravel island (Q_{over} = 0.5–1.5 l m^{-1} s^{-1};

Figure **3e**) than the sand island (Q_{over} = 1–2.4 l m^{-1} s^{-1}; Figure **3j**), and increasing with rate of SLR. The fluctuations in Q_{over} values, despite applying a 5-hr moving average, occur because the hourly wave forcing varies stochastically as a new wave signal is generated at the start of each hour. There is less difference between the simulations with 100 and 200 hr of wave action, than between those with 50 and 100 hr of wave action, especially for the gravel island; therefore, and for reasons of expediency (a 100-hr morphodyamic simulation takes 100 hrs computing time on a 4-core Windows machine), a rate of SLR of 0.01 m per hr^{-1} of wave action was used in the remaining simulations.

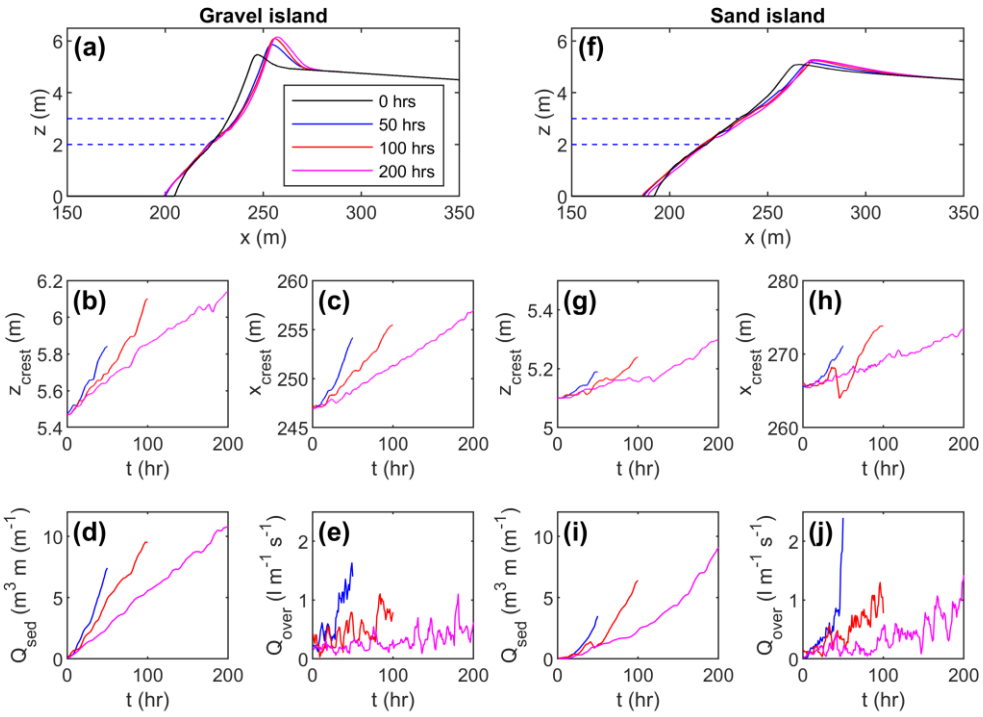

Figure **3** – Modelled evolution of the gravel (left panels; a–e) and sand (right panels; f–j) reef island during a 1-m SLR (from h = 2 m to 3 m) with rates of SLR of 0.02 m, 0.01 m and 0.005 m per 1 hr of wave action with constant wave forcing of H_0 = 3 m, T_p = 9.9 s. (a, f) Island morphology at the start and end of model simulation, and time series of (b, g) island crest elevation z_{crest}, (c, h) island crest position x_{crest}, (d, i) cumulative sediment transport Q_{sed} across the island crest and (e, j) overwash discharge Q_{over} across the island crest. Note the different y-axis scales for (b) and (g), and (c) and (h). The time series were smoothed using a 5-hour moving window. [p_SLR_axes]

3.2 Role of reef growth on island response to sea-level rise

A 2.5-m SLR rising at 0.01 m hr^{-1} of wave action was used to investigate the role of reef growth on gravel and sand island response (**Test D**; Table **1**). Animations of the island response for the gravel and sand islands with a static reef are visualized in Movies **S1** and **S2**. For the first 1.5 m of SLR from +2.0 to +3.5 m (t = 150 hrs), there was no significant difference in island evolution or overwash discharge between the simulations with and without reef growth (Figure **4**). Both gravel and sand island accreted and retreated, but the gravel island accreted more (Δz_{crest} = 0.8 m; Figure **4b**) than the sand island (Δz_{crest} = 0.4 m; Figure **4g**), and the sand island underwent more retreat (Δx_{crest} = 20 m; Figure **4h**) than the gravel island (Δx_{crest} = 10 m; Figure **4c**). For both islands, the amount of SLR exceeded the change in z_{crest}; therefore, the amount of freeboard (z_{crest}-SWL) decreased, and this resulted in an increase of the overwash discharge Q_{over} (Figure **4e,j**).

During the last 100 hrs of the simulations, when sea level increased from +3.5 to +4.5 m, the gravel island without reef growth continued to accrete and retreat, maintaining a freeboard of 3 m with Q_{over} increasing from 2 to 4 l m^{-1} s^{-1} (Figure **4d,e**). With reef growth, the gravel island also continued to accrete, but slightly less, attaining a freeboard

of 2.5 m at the end of the simulation. Over the same period, the sand island without reef growth also continued to accrete and retreat, albeit at reduced and increased rate, respectively, and with freeboard reducing to 1.5 m and Q_{over} increasing from 5 to 20 l m^{-1} s^{-1} (Figure **4i,j**). With reef growth, the sand island started to fail after 150 hrs, and by the end of the simulation only 0.5 m freeboard remained with Q_{over} > 50 l m^{-1} s^{-1}. The rate of retreat of the sandy island during the first 1 m SLR is relatively limited (< 0.1 hr^{-1}), but then rapidly acceletrates to almost 1 m hr^{-1} over the remainder of the simulation (Figure **4h**).

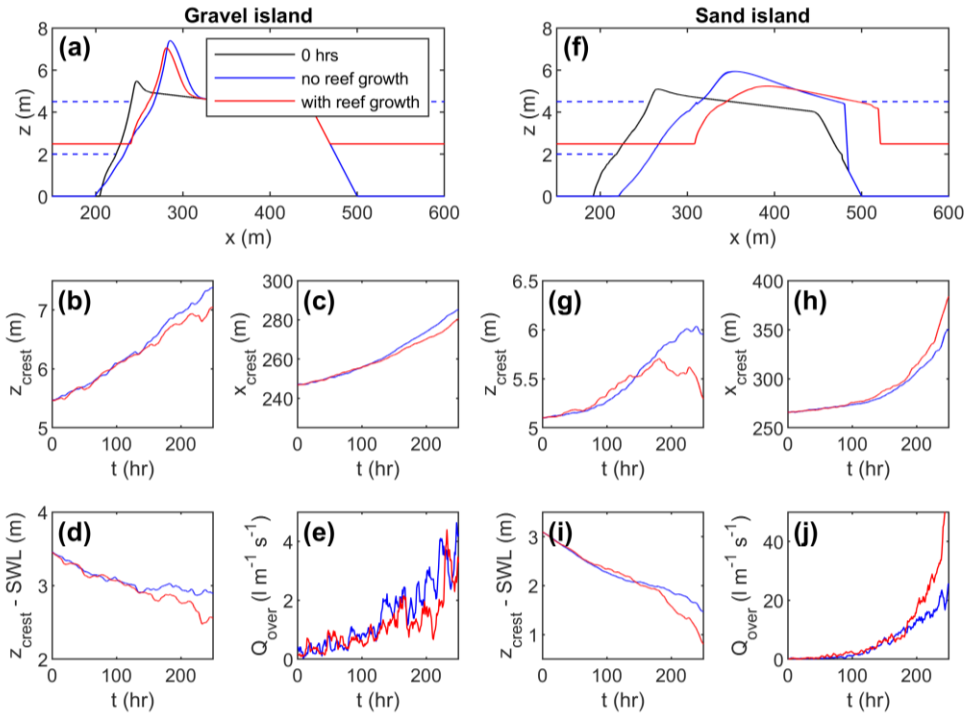

Figure **4** – Modelled evolution of the gravel (left panels; a–e) and sand (right panels; f–j) reef island during a 2.5-m SLR with (blue lines; +RG) and without (red lines; -RG) reef growth keeping pace with rising sea level, and with constant wave forcing of H_0 = 3 m and T_p = 9.9 s. (a, f) Island morphology at the start and end of model simulation, and time series of (b, g) island crest elevation z_{crest}, (c, h) island crest position x_{crest}, (d, i) freeboard z_{crest}-SWL and (e, j) overwash discharge Q_{over} across the island crest. Note the different y-axis scales for the gravel (b–e) and sand (g–j) island. The time series were smoothed using a 5-hour moving window. [p_reef_growth_axes_V2]

3.3 Hydrodynamics during sea-level rise

The results indicate that, overall, reef growth does not appear to offset the physical impacts of SLR and make the reef islands more resilient. This result is somewhat surprising as it challenges prevailing insights on the importance of reef structure in affording some protection to island shorelines (Ferrario et al., 2014). Consequently, this result is further investigated through consideration of the hydrodynamics during the simulations. Using four different morphological boundary conditions (unmodified (–M) and modified (+M) island morphology; with (+RG) and without (–RG) reef platform growth), hourly-averaged hydrodynamics were computed using XBeach-G for every 10th hour of the 2.5-m SLR simulations (i.e., t = 0, 10, 20, 30, … hrs, or SLR = 0, 0.1, 0.2, 0.3, … m; **Test E**; Table **1**). The wave setup η, significant wave height H_s and incoming infragravity significant wave height $H_{s,inf,in}$ (computed using Guza and Thornton, 1984) at the toe of the beach (at x = 190 m), and the overwash discharge Q_{over} across the island crest were extracted from the modelled data, and are plotted as a function of the amount of SLR in Figure **5**.

Wave conditions at the toe of the beach for the simulations with static reef platform (-RG), regardless of whether the island morphology is constant (no morphodynamic updating during model simulations; -M) or modelled (with morphodynamic updating; +M), are very similar and vary in a consistent manner with increasing sea level in line with Figure **S1** (solid lines in Figure **5b,c,d,e,g,h,i**). Wave conditions at the toe of the beach remain relatively constant if the reef platform keeps pace with SLR (dashed lines in Figure **5b,c,d,e,g,h,i**). As expected, the beach

morphology has limited influence on the wave conditions across the reef platform. The overwash discharge across the island crest Q_{over} increases with SLR for all simulations (Figure **5f,j**). For the unmodified gravel and sand island, Q_{over} > 1 l m^{-1} s^{-1} after 1-m SLR, but Q_{over} does not exceed 10 l m^{-1} s^{-1} if the reef platform keeps pace with SLR (+RG). This is especially apparent for the gravel island with the difference between reef growth and no growth increasing with SLR. For an evolving island, Q_{over} is much smaller than for the unmodified island, at least by up to one order of magnitude by the end of the simulation; however, the Q_{over} values for with and without reef growth are very similar. The beach morphology has thus significant influence on the overwash characteristics.

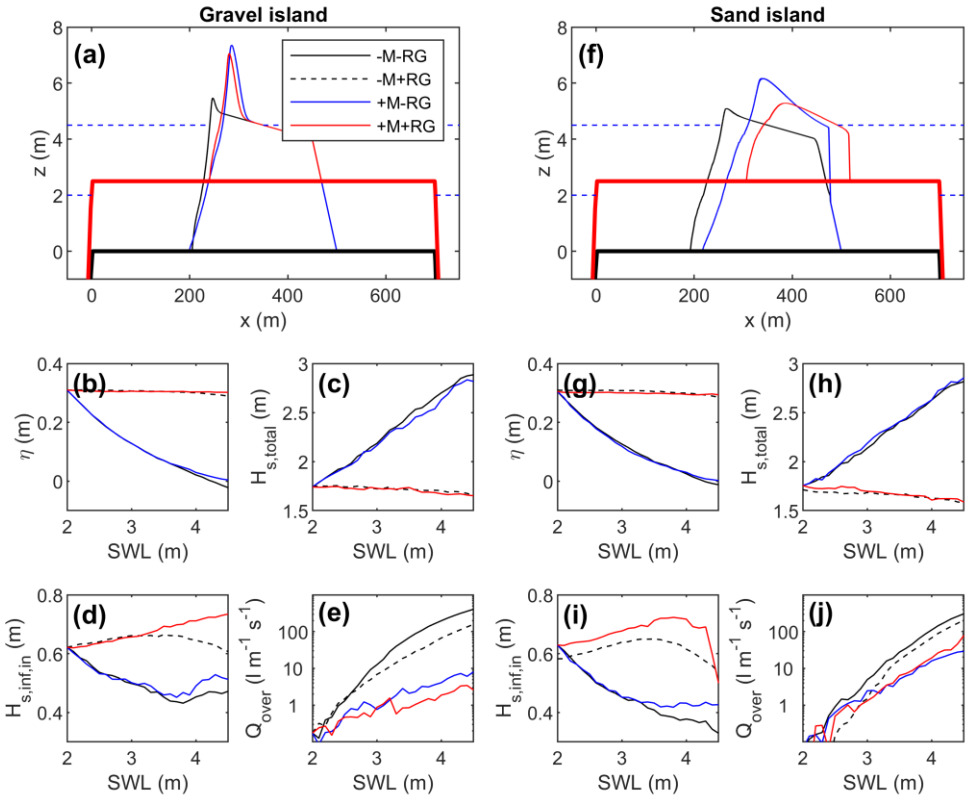

Figure **5** – Modelled evolution and associated hydrodynamics of the gravel (left panels; a–e) and sand (right panels; f–j) reef island during a 2.5-m SLR with (+RG) and without)-RG) reef growth keeping pace with rising sea level, and with constant wave forcing of H_0 = 3 m, T_p = 9.9 s. (a, f) Island morphology at the start and end of model simulation, and time series of (b, g) wave setup η, (c, i) significant wave height H_s, (d, i) incoming infragravity significant wave height $H_{s,inf,in}$ and (e, j) overwash discharge Q_{over} across the island crest. The time series represent hourly averages for every 10 hrs of the 250-hr simulation, and on the *x*-axis the SWL plotted rather than the time (SWL = 0 m represents level of the reef platform at start of simulation). Bold lines represent reef platform. The different runs represent: +M = evolving island; -M = unmodified island; +RG = with reef growth; and –RG = without reef growth. [p_hydro_axes_V2]

If the morphological response of the island to SLR is ignored, then reef growth significantly reduces overwash discharge and coastal flooding, because the shallower water depths across the reef enhance wave energy dissipation and reduce wave runup, whilst at the same time maintaining wave set-up and infragravity wave action (cf., solid and black dashed lines in Figure **5**). In that case, platform growth contributes positively to island resilience and helps mitigate the physical impacts of SLR. For an evolving island, however, the overwash discharge, and therefore the extent of coastal flooding and island inundation, does not depend greatly on whether the reef platform grows or not (cf., solid red and blue lines in Figure **5e,j**). This can be explained by considering that, according to the numerical model, the island elevation adjusts to SLR such that z_{crest} matches more or less the maximum runup height $R_{2\%}$. Smaller h_{reef} values for a reef that keeps up with SLR therefore result in lower islands. The failure of the sandy island with reef growth compared to the one without reef growth at the end of the simulation is puzzling. It is suggested that the higher wave setup η and incoming infragravity significant wave height $H_{s,inf,in}$ in the former case is less conducive to island maintenance than the higher significant wave height H_s in the latter case.

3.4 Dependence of island response to wave height

So far, only a single wave conditions (H_0 = 3 m) has been used for the morphodynamic SLR simulations and this wave condition has been selected on the basis of the wave runup it generates on the initial island morphology (cf., Figure 2). More energetic conditions are considered to be too infrequent to play a role in the elevation of the island and less energetic conditions do not reach the crest and can therefore not modify the top of the island. However, as island freeboard decreases, e.g., by the end of the 2.5-m SLR simulation of the sand island, less energetic wave conditions (H_0 < 3 m) should become increasingly able to reach the island crest and contribute positively to island maintenance. Similarly, more energetic wave conditions (H_0 > 3 m) should be come increasingly destructive due to the larger overwash discharge. To illustrate such shift in wave height thresholds between 'neutral', 'constructive' and 'destructive' wave conditions, XBeach models were set-up using the gravel and sand island morphology that developed after 2-m SLR accounting for reef growth (i.e., morphology developed at t = 200 hrs in **Test D**; Table 1), and offshore wave conditions ranging from of H_0 = 1 m to 5 m in 0.1-m steps (**Test F**; Table 1). A sea level of 4.5 m, representing a SLR of 2.5 m, was used to deliberately reduce the island freeboard by 0.5 m to bring out the role of wave height in island development. The change in island morphology (dz_{crest} and dx_{crest}) and overwash characteristics (mean overwash depth h_{crest} and discharge Q_{over} across the island crest) for each 1-hr simulation was computed and plotted as a function of H_0 (Figure 6).

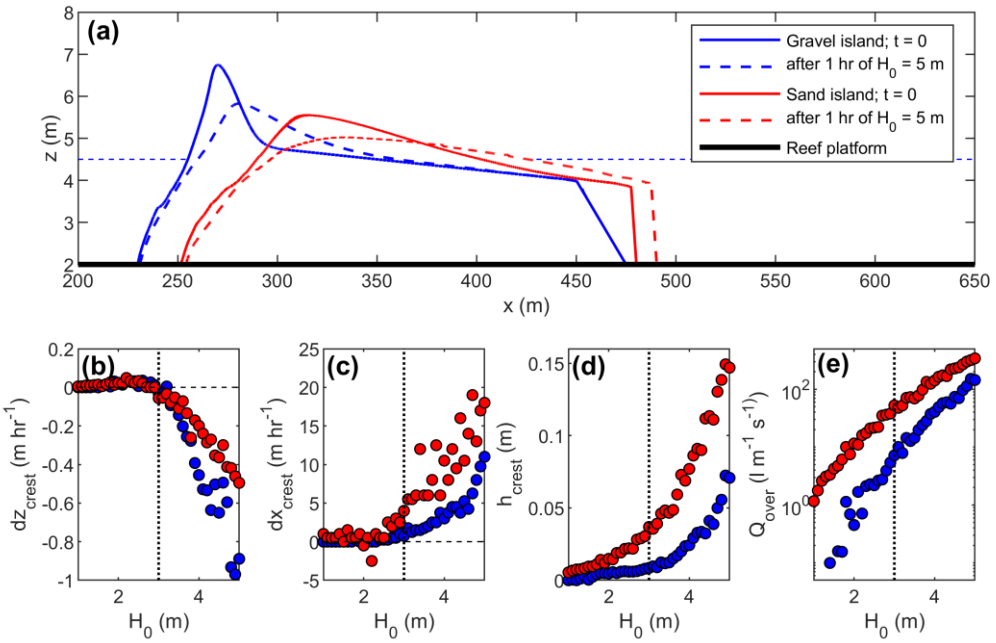

Figure 6 – (a) Gravel and sand island morphology after 2 m SLR at t = 200 hrs during **test D**, but with with sea level and reef platform representing a SLR of 2.5 m, which was subjected to offshore wave conditions increasing from H_0 = 1 m to 5 m in 0.1-m steps for 1 hr for each wave conditions. Dashed lines show island morphology after 1 hr of H_0 = 5 m. Lower panels show relationship, for gravel (blue circles) and sand (red circles) island, between offshore wave height H_0 and: (b) change in crest elevation dz_{crest}; (c) change in crest position dx_{crest}; (d) average water depth h_{crest} across island crest; and (e) overwash discharge Q_{over} across island crest. The vertical dotted line at H_0 = 3 m represents the approximate wave height threshold between island crest building and destruction. Mean h_{crest} is computed over the whole simulation, including zeros when dry. [p_H_threshold_axes]

The results for both 'underfit' islands, i.e., islands with significantly reduced freeboard compared to the start of the simulation, indicate that raising of the island crest (dz_{crest} > 0) occurs for all wave conditions characterised by H_0 < 3 m, while the crest location remains relatively constant (dx_{crest} < 3 m; Figure 6b,c). Such wave conditions correspond to hydrodynamic thresholds of dh_{crest} = 0.01 m and Q_{over} = 5 l m^{-1} s^{-}1 for the gravel island, and dh_{crest} = 0.03 m and

Q_{over} = 20 l m^{-1} s^{-1} for the sand island (Figure **6d,e**). For H_0 > 3 m, the island crest is lowered and retreats with increasing H_0. Subjecting the gravel island to H_0 = 5 m for only one hour, results in a decrease in crest height of 1 m and crest retreat of 10 m, and is associated with h_{crest} = 0.08 m and Q_{over} = 150 l m^{-1} s^{-1}. For the sand island, dz_{crest} = -0.5 m and dx_{crest} = 20 m, and h_{crest} = 0.15 m and Q_{over} = 350 l m^{-1} s^{-1}. It thus appears that the crest of the gravel barrier is morphologically more responsive to destructive wave conditions than the crest of the sand island, despite the smaller overwash depths and discharge; but, on the sand island, overwash occurs across the entire island resulting in washover deposits behind the barrier (i.e., complete washover; Figure **6a**). Animations of the overwash characteristics at either side of the H_0 = 3 m threshold are visualized in Movies **S3** and **S4**.

3.5 Considering the full energetic part of the wave climate (H_0 *> 2 m)*

In the final set of simulations, gravel and sand island response to a 2.5-m SLR at a rate of 0.01 m hr^{-1}, and accounting for reef growth, was modelled, with variable wave conditions (H_0 = 2–5 m; **Test G**; Table **1**). The gravel island continues to accrete and retreat during SLR, whilst retaining freeboard (Figure **7a,b**), and the final morphology is actually quite similar to the simulation with constant wave conditions (cf., Figure **6a,b**). In contrast, the sand island initially accretes modestly and retreats up to t = 150 hrs (1.5-m SLR), but then rapidly looses freeboard and shows 'run-away' migration, becoming permanently submerged after t = 200 hrs and with all sediment transferred into the lagoon by the end of the simulation (Figure **7e,f**). In the simulations with constant wave conditions and reef growth, the sand island also starts to 'fail' around t =150 hrs (cf., Figure **7f,g**), but not as spectacular as with variable wave conditions. The disparate trajectories of the gravel and sand island are directly linked to the overwash discharges across the island crest with Q_{over} < 20 l m^{-1} s^{-1} throughout the simulation for the gravel island and Q_{over} > 100 l m^{-1} s^{-1} after t = 150 hrs for the sand island (Figure **7c,g**).

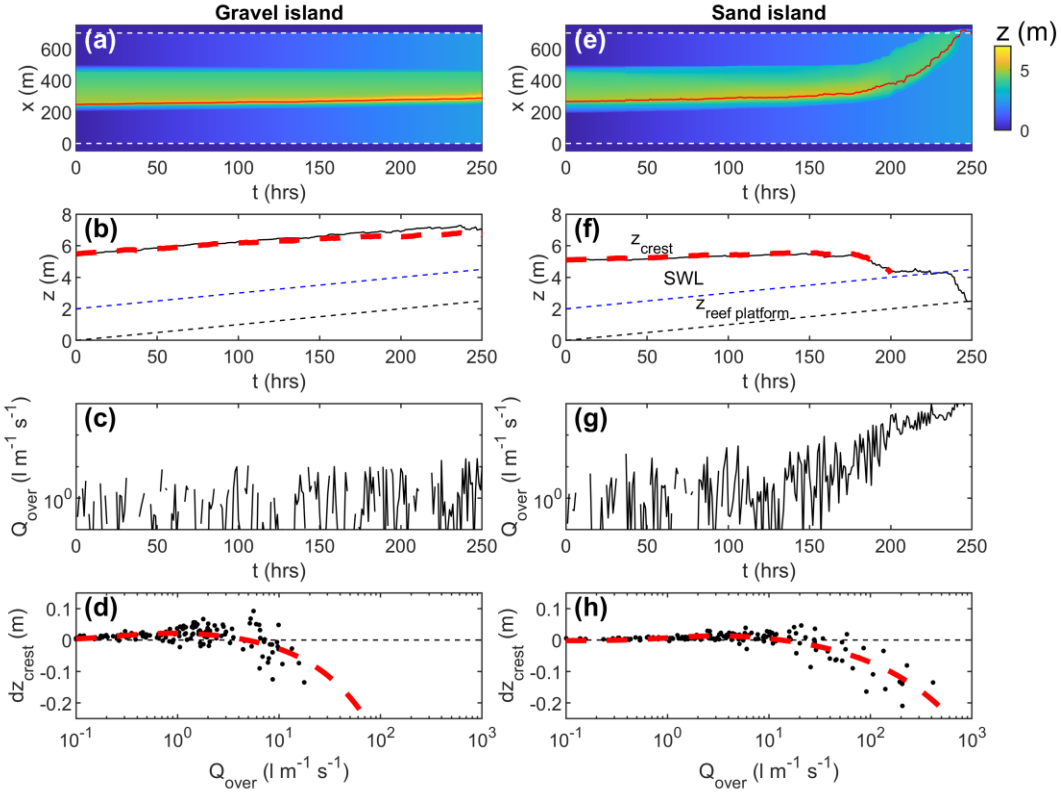

Figure **7** – Modelled evolution of the gravel (left panels; a–d) and sand (right panels; e–h) reef island during a 2.5-m SLR with reef growth keeping pace with rising sea level, and with variable wave forcing of H_0 = 2–5 m and T_p = 9.9 s. (a, e) Evolution of island morphology with colour representing elevation, red line indicating position of island crest and horizontal white dashed lines representing edge of reef platform. (b, f) Time series of island crest elevation z_{crest}, still water level SWL and elevation of reef platform $z_{reef\ platform}$; red dashed line

represents z_{crest} predicted using the fitted line to the data in (d) and (h). (c, g) Time series of overwash discharge across the island crest Q_{over} with gaps in the time series indicating wave runup did not reach the island crest (i.e., Q_{over} = 0). (d, h) Scatter plots of Q_{over} *versus* hourly change in island crest elevation dz_{crest} with the red dashed line representing the best fit line. [p_varH]

During the run with variable wave conditions, z_{crest} increases and decreases depending on the energy level of the wave conditions driving the amount of overwash. To explore this relation in more depth, Figure **7d, h** relates Q_{over} to the hourly change in island crest elevation dz_{crest}, where each data point represents one hour of variable forcing (H_0 = 2–5 m). A similar plot was presented earlier where dz_{crest} was related to H_0 using results of **test F** (cf., Figure 7). For both the gravel and sand island, the model data show positive dz_{crest} values for relatively small values of Q_{over}, and negative dz_{crest} values for relatively large values of Q_{over}, with a threshold value for Q_{over} of 5 l m^{-1} s^{-1} and 20 l m^{-1} s^{-1} for gravel and sand island, respectively. An equation was fitted to the data of the form:

$$d_{z,crest} = [a_1 tanh(b_1 \log Q_{over} + c_1) + a_1] + [a_2 \exp(b_2 \log Q_{over} + c_2)] \quad \textbf{(Eq. 1)}$$

where [a_1, a_2, b_1, b_2, c_1, c_2] are fitting coefficients (gravel = [1/50, -1/94, 1.7, 1.7, 0.85, 0.15 with r^2 = 0.36]; sand = [1/50, -1/70, 1.6, 1.2, -0.15, -0.35 with r^2 = 0.69]). The first and second term in the Eq. 1 represent the crest accretion ($d_{z,crest} > 0$) and crest erosion ($d_{z,crest} < 0$) part of the data, respectively. Despite considerable scatter, application of Eq. 1 to predict the evolution of $d_{z,crest}$ as a function of the hourly mean overwash discharge Q_{over} matches the numerical model output quite well (Figure **7b** for gravel island; Figure **7f** for sand island).

4 Discussion

Masselink et al. (2020) introduced the numerical model approach used in the present paper and demonstrated that coral reef islands composed of gravel have the potential to vertically accrete in reponse to a 1-m SLR to retain freeboard, confirming physical modelling (Tuck et al., 2019a, 2019b). This ability of islands to vertically accrete under energetic wave and/or water level forcing has also been demonstrated by field observations (Kench et al. 2006; Hoeke et al., 2013; Kench and Beetham, 2019). The model results of Masselink et al. (2020) also showed that the maximum increase in island elevation was associated with a mean crest discharge of 0.01–0.02 m^3 m^{-1} s^{-1} (10–20 l m^{-1} s^{-1}), with higher discharge magnitudes resulting in crest lowering. This paper confirms and significantly extends these results; specifically, we have now also considered the response of sand islands, extended the magnitude of SLR to 2.5 m, evaluated the role of future reef growth on island response, and explored the importance wave height variability. We stress that our simulations purposely adopted higher magnitudes of SLR (representing >100-year time horizon) and wave energies to purposely evaluate morphological behaviours and critical thresholds that denote changes in physical response to boundary process conditions.

4.1 Limitations

Despite the sophistication of the processed-based model used here, accounting for wave-resolving hydrodynamics and swash-groundwater interactions, there are many factors that also play an important role in driving and/or controlling reef island response to SLR that have not been considered. These include the influence of: temporally-varying rates of SLR which may afford differential relaxation periods for morphological response; width, shape and roughness of the reef platform on wave transformation processes (Quataert et al., 2015; Pearson et al., 2017); the potentially stabilizing role of island vegetation (Duvat and Pillet, 2017); island infrastructure providing obstructions and/or conduits for overwash on inhabited islands (Duvat and Magnan, 2019); and sediment supply to the island (gravel and sand) from the reef system (Gischler and Lomando, 1999; Perry et al., 2011; Dawson and Smithers, 2014; Kayanne et al., 2016). It is also relevant to point out that only the gravel island model settings have been validated with the small-scale physical experiment reported in Tuck et al. (2019b) and that, to date, there has been no validation of the sand island model. Additonally, identical starting morphology and position for the gravel and sand island on the reef platform is not realistic, as gravel islands tend to be higher and are generally located at more exposed locations on the platform than sand islands (Stoddart and Steers, 1977). Nevertheless, despite the simplified representation of the reef-island topography and the exclusion of several important factor and processes in the modelling approach, the key results of this modeling study are insightful and merit further discussion. An additional limitation is the simplification of island and reef morphology to a 1D profile that does not account for wave refraction and alongshore sediment transport; however, Tuck et al. (2019a) demonstrated in their wave basin

experiment that the central island profile of their 2D island behaved very similar to SLR to the island profile in a wave flume.

4.2 Gravel versus *sand island response*

Both gravel and sand islands show vertical accretion in response to SLR (cf., Masselink et al., 2020), but the model results suggest that the gravel island is better able to retain freeboard than the sand island, and could be considered more resilient to SLR. This is evident by the end of the 2.5-m SLR simulation, when, if reef growth is ignored, the elevation of the gravel island crest level increased by almost 2 m, while the sand island crest was only raised by c. 1 m (cf., Figure **4**). If reef growth is considered, the difference between gravel and sand island response to a 2.5-m SLR is even more pronounced: the gravel island accreted 1.5 m, whereas the sand island was almost destroyed by the end of the simulation (cf., Figure **4**). If a variable wave climate is used and reef growth is considered, the sand island is completely destroyed by the end of the 2.5-m SLR simulation, while the gravel island retains more than 1.5 m freeboard by the end of the simulation (Figure **7**).

The difference in response to SLR between gravel and sand islands can be explained, in part, by wave runup and overwash characteristics, and also overwash infiltration losses, as they were modelled in the simulations. The lower elevation of the modelled sand island is directly related to the fact that sandy beaches have gentler beach gradients than gravel beaches (Bujan et al., 2019). A gentler beach gradient reduces wave runup height (Stockdon et al. 2006; Poate et al., 2016) and the ability of the waves to vertically construct the island as island crest level is 'tuned' by the maximium runup elevation. The lower elevation and less resilient behavior of the sand island is also attributed to the larger transportability and smaller hydraulic conductivity of sand-sized material compared to gravel. On the modelled sand island, all overwash flowed down the backslope of the island to the lagoon. As the back-slope is relatively constant, high flow velocities and transport rates are maintained, limiting sediment deposition around the island crest and causing accretion to occur across the entire width of the island and in the form of washover deposits, as also documented in field observations (e.g., Leatherman, 1979; McCall et al., 2010; Matias et al., 2016). In contrast, the gravel material is more resistant to movement and has a high hydraulic permeability. Overwash water will be rapidly lost through infiltration after passing the island crest and this will result in localized sediment accretion around the crest location, without any water or sediment flowing across the back of the island (e.g., Matias, et al., 2012). These are relevant and very fundamental differences between gravel and sand islands, and they are likely to respond very differently to SLR. Another factor not considered in the modelling approach is the presence of island vegetation, which might me especially relevant for the generally densely vegetated sand islands. Vegetation not only slow down the flows, but also acts to stabilize the surface of the island; both factors are expected to increase island resilience.

4.3 Role of future reef growth

Model results suggest that, for an evolving island, reef growth has little influence on overwash discharge, coastal flooding and island inundation. In other words, reef growth does not seem to make the islands more resilient to SLR. This is a surprising finding and counter-intuitive given the protective role widely bestowed upon reef platforms. However, such assertions have previously been based on hydrodynamic modelling studies conducted for static and non-changing island structures (Quataert et al., 2015; Beetham et al., 2017; Pearson et al., 2017). The difference between previous model studies and the current one arises because in the present morphodyamic modelling approach, the island adjusts morphologically to SLR such that z_{crest} matches more or less the maximum runup height $R_{2\%}$, with the latter largely a function of incident wave forcing H_0 and water depth across the reef platform h_{reef} (cf., Figure **1**). In case of a progressively deepening reef platform during SLR (i.e., without platform growth), the increasingly energetic swash regime will drive higher wave runup, leading to a more elevated island crest. If the reef platform keeps pace with SLR (i.e., with platform growth), the swash regime remains relatively benign and, even though the island crest will still vertically accrete during SLR, z_{crest} will remain lower than in the case of a static reef platform elevation (cf., Figure **4a,b,f,g**). Conversely, if island adjustment is not included in the model, or not possible in reality due to topographic or anthropogenic constraints (e.g., seawall), reef platform growth does contribute positively to island resilience as suggested by previous hydrodynamic studies (Quataert et al., 2015; Beetham et al., 2017; Pearson et al., 2017), because the constant h_{reef} during SLR continuous to dissipate incoming wave energy, limiting wave runup, overwash discharge and coastal flooding. Hydrodynamic and morphodynamic models can thus yield contradicting results.

4.4 Impact of wave height variability

A single wave height value of H_0 = 3 m was used in most simulations and its choice was informed by exposing the idealized island morphology to a range of wave conditions and selecting the wave height that just overtopped the island crest. A value of H_0 = 3 m happens to reflect a wave height that roughly corresponds to the 99% exceedance wave height for portions of the tropical Pacific as modelled by the Changing Waves and Coasts in the Pacific project (WACOP.gsd.spc.int), so reflects an energetic wave condition that can be expected to occur at high tide a few times per year in this region, but perhaps only once a year during spring high tide. There are many coral reef islands, however, that experience either more (e.g., Marshall Islands; Storlazzi et al., 2018) or less (e.g., Wadey et al., 2017; Maldives;) energetic wave conditions; therefore, the role of different wave conditions (H_0 = 2 to 5 m), including the occurrence of tropical cyclone waves every few years to decades, was considered in the final set of simulations, whilst also considering reef growth. The response of the gravel island to 2.5-m SLR with variable wave conditions was very similar to using constant wave conditions, but the sand island was completely eroded by the end of the simiulation with variable wave conditions (cf., Figure **7**). The most useful aspect of these simulations is that it exposes the reef island to hourly fluctuations in the overwash discharge Q_{over} that can be correlated to the hourly change in island crest elevation dz_{crest}. The gravel and sand island vertically accrete ($dz_{crest} > 0$) as long as $Q_{over} < 5$ l m^{-1} s^{-1} and < 20 l m^{-1} s^{-1}, respectively.

There is considerable scatter in the $Q_{over} - dz_{crest}$ plots based on the simulations with variable wave forcing (Figure **7d,h**), but fitted lines explain a considerable amount of variability in the data. These fitted equations were implemented to provide an alternative means to model the evolution of the island crest elevation statistically by using only the hourly-averaged Q_{over}. The results obtained from application of the statistical model show good agreement with the numerical model results (Figure **7b,f**). This analysis perhaps points towards a way to model island evolution, at least the evolution of the island crest, taking into account the full wave climate and water level variability. Such approach could involve: (1) using the BEWARE or a similar data set to predict overwash discharge across the crest as a function of reef-island topography (reef width, roughness, island elevation and beach slope), water depth a aross the reef platform and wave conditions (height and period) (as per Figure **1**); (2) use XBeach to create a data set to predict crest change from overwash discharge for different island geometries and sedimentologies; and (3) combine (1) and (2) into a simple model forced by a very large number of realisations of H_0, T_p and h_{reef} time series to predict the long-term evolution of the island crest elevation.

4.5 Implications

The results show that coral reef islands can vertically accrete via flooding and overwash if specific oceanographic and sedimentary conditions exist, and this notion should be taken into account when considering the future of these islands. In particular, our simulations that assume a finite sediment reservoir, high magnitude SLR and energeic wave conditions, present a worst-case set of constraints on island response. Consequently, results underscore considerable island resilience. In addition, anthropogenic activities that disrupt the natural sedimentary system, such as coastal defence works, will require careful consideration as, on the one hand they prevent flooding that can negatively impact infrastructure, freshwater availability, agriculture and terrestrial habitats, but on the other hand these measures also prevent the island from naturally adjusting through overwash deposition. Ultimately, our findings suggest that uninhabited or sparsely populated islands can physically adjust to a point beyond which they can grow no higher under assumptions of lack of sediment supply and/or changes in storm wave frequency occur that are conducive to islands flattening. However, heavily urbanised islands, the same processes will drive island change will negatively impact infrstructure and assets.

The findings also highlight that future trajectories of coral reef islands will also be influenced by coral reef ecology, specifically future reef platform accretion rates and reef sediment production/delivery to the reef islands. As shown in this study, adjustments in reef level will modify wave processes and interactions with an evolving shoreline. However, future reef growth trajectories still remain uncertain. Future SLR may outpace new reef flat accretion at many sites, resulting in an increase in water depth over coral reefs (Perry et al., 2018), although the exact magnitude is unclear. Our results show possible island responses in the absence of new inputs of detrital sediment. Intuitively, the addition of sediment should positively influence island physical response and resilience, though knowledge of the rates of sediment generation, the temporal variability in sediment generation and its delivery to islands are poorly constrained (Perry et al., 2012; Yates et al., 2017). While new supplies of sediment are necessarily reliant on a healthy reef state over decadal timescales, many reefs are subject to anthropogenic stresses that may reduce

carbonate sediment production that feeds coral reef islands (Perry et al., 2012). Better constraining carbonate sediment production, sediment delivery from the coral reefs to the islands and how climate change and SLR may affect those processes (e.g., Storlazzi et al., 2011; East et al., 2020) are key to better forecasting how coral reef islands may evolve in the following decades (Winter et al., 2020).

5 Conclusions

A process-based numerical model was used to simulate the morphological response of gravel and sand coral reef islands to sea-level rise (SLR) and investigate the role of future reef growth on island response.The model results indicate that reef islands can evolve during SLR by accreting to maintain positive freeboard while retreating lagoonward by means of overwash. As long as the mean overwash discharge across the island crest remains below a certain threshold $O(10\ \mathrm{l\,m^{-1}\,s^{-1}})$, islands accrete vertically during sea-level rise. A larger overwash discharge results in lowering of the island which can ultimately lead to island destruction under extreme forcing scenarios. Although the presence of a shallow reef platform in front of an island significantly reduces the wave energy incident at the island shoreline, due to wave breaking across the platform, model outputs show future reef growth does not increase the ability of islands to adjust to sea-level rise on the medium-term (< 50 years). This is because the maximum elevation of reef islands that keep pace with SLR, and thus maintain positive freeboard, is attuned to the maximum wave runup. Thus, islands fronted by a growing reef platform that keeps pace with SLR attain lower elevations than those without reef growth due to reduced wave energy at the shoreline, but will have a similar overwash regime. The model also indicates that, for the same oceanographic forcing, gravel islands build up higher than sand islands due to their steeper beachface gradient leading to higher runup. In conclusion, islands can grow vertically to keep up with SLR via flooding and overwash if specific forcing and sediment supply conditions are met, offering hope for uninhabited and sparely populated islands; however, on urbanised islands, mechanisms driving physical island response will negatively impact infrastructure and assets.

Acknowledgements

GM would like to acknowledge the support of EPSRC Overseas Travel Grant EP/T004304/1.

References

Beetham, E. and Kench, P.S. (2018), A global tool for predicting future wave-driven flood trajectories on atoll islands. *Nature Communications*, *9*, 3997, https://doi.org/10.1038/s41467-018-06550-1.

Beetham, E., Kench, P.S. and Popinet, S. (2017), Future reef growth can mitigate physical impacts of sea-level rise on atoll islands. *Earth's Future*, 5, 1002–1014, https://doi.org/10.1002/2017EF000589.

Brander, R.W., Kench, P.S. and Hart, D. (2004), Spatial and temporal variations in wave characteristics across a reef platform, Warraber Island, Torres Strait, Australia. *Marine Geology*, *207*, 169–184, https://doi.org/10.1016/j.margeo.2004.03.014.

Brown, B.E., Dunne, R.P., Phongsuwan N. and Somerfield, P.J. (2011), Increased sea level promotes coral cover on shallow reef flats in the Andaman Sea, eastern Indian Ocean, *Coral Reefs*, *30*, 867, https://doi.org/10.1007/s00338-011-0804-9.

Cheriton, O., Storlazzi, C.D. and Rosenberger, K. (2016), Observations of wave transformation over a fringing coral reef and the importance of low-frequency waves and offshore water levels to runup, overwash, and coastal flooding, *Journal of Geophysical Research (Oceans)*, *121*, 3121–3140, https://doi.org/10.1002/2015JC011231.

Dawson, J.L. and Smithers, S.G. (2014) Carbonate sediment production, transport, and supply to A coral cay at Raine Reef, Northern Great Barrier Reef, Australia: a facies approach. *Journal of Sedimentary Research*, *84*, 1120–1138, http://dx.doi.org/10.2110/jsr.2014.84.

Duvat, V.K.E. and Magnan, A.K. (2019), Rapid human-driven undermining of atoll island capacity to adjust to ocean climate-related pressures, *Scientific Reports*, *9*, 15129, https://doi.org/10.1038/s41598-019-51468-3.

Duvat, V.K.E. and Pillet, V. (2017), Shoreline changes in reef islands of the Central Pacific: Takapoto Atoll, northern Tuamotu, French Polynesia. *Geomorphology*, *282*, 96–118, https://doi.org/10.1016/j.geomorph.2017.01.002.

East, H.K., Perry, C.T., Beetham, E.P., Kench, P.S. and Liang, Y. (2020) Modelling reef hydrodynamics and sediment mobility under sea-level rise in atoll reef island systems. *Global and Planetary Change*, *192*, 103196, https://doi.org/10.1016/j.gloplacha.2020.103196.

Ferrario, F., Beck, M.W., Storlazzi, C.D., Micheli, F., Shepard, C.C. and Airoldi, L. (2014), The effectiveness of coral reefs for coastal hazard risk reduction and adaptation. *Nature Communications, 5*, 3794, https://doi.org/10.1038/ncomms4794.

Gischler, E. and Lomando, A.J. (1999) Recent sedimentary facies of isolated carbonate platforms, Belize-Yucatan system, Central America. *Journal of Sedimentary Research*, 69, 747–763, https://doi.org/10.2110/jsr.69.747.

Guza, R.T. and Thornton, E.B. (1985), Observations of surf beat, *Journal of Geophysical Research (Oceans)*, *90*, 3161–3172, https://doi.org/10.1029/JC090iC02p03161.

Hoegh-Guldberg, O. (1999), Climate change, coral bleaching and the future of the world's coral reefs, *Marine and Freshwater Research*, *50*, 839–866, https://doi.org/10.1071/MF99078.

Hoeke, R., McInnis, K.L., Kruger, J.C., McNaught, R.J., Hunter, J.R. and Smithers, S.G. (2013), Widespread inundation of Pacific islands triggered by distant-source wind-waves, *Global and Planetary Change, 108*, 128–138, https://doi.org/10.1016/j.gloplacha.2013.06.006.

Hughes, T.P. et al. (2017), Global warming and recurrent mass bleaching of corals, *Nature, 543*, 373–377, https://doi.org/10.1038/nature21707.

Kayanne, H., Aokei, K., Suzuki, T., Hongo, C., Yamano, H., Ied, Y., Iwatsuka, Y., Takahashi, K., Katayama, H., Sekimoto, T. and Isobe, M. (2016) Eco-geomorphic processes that maintain a small coral reef island: Ballast Island in the Ryukyu Islands, Japan. *Geomorphology*, *271*, 84–93, https://doi.org/10.1016/j.geomorph.2016.07.021.

Kench, P.S. and Beetham, E.P. (2019), Evidence of vertical building of reef islands through overwash and implications for island futures, *Proceedings Coastal Sediments'19*, ASCE, Tampa, USA, 916–929.

Kench, P.S., Beetham, E., Bosserelle, C., Kruger, J., Pohler, S., Coco, G. and Ryan, E. (2017), Nearshore hydrodynamics, shoreline sediment fluxes and morphodynamics on a Pacific atoll Motu, *Marine Geology, 389*, 17–31, https://doi.org/10.1016/j.margeo.2017.04.012.

Kench, P.S., McLean, R.F., Brander, R.W., Nichol, S.L., Smithers, S.G., Ford, M.R., Parnell, K.E. and Aslam, M. (2006), Geological effects of tsunami on mid-ocean atoll islands: The Maldives before and after the Sumatran tsunami, *Geology*, *34*, 177–180, https://doi.org/10.1130/G21907.1.

Kench, P.S., Parnell, K.E. and Brander, R.W. (2009), Monsoonally influenced circulation around coral reef islands and seasonal dynamics of reef island shorelines, *Marine Geology*, *266*, 91–108, https://doi.org/10.1016/j.margeo.2009.07.013.

Leatherman, S. P. (1979) Migration of Assateague Island, Maryland, by inlet and overwash processes. *Geology*, 7, 104-107, https://doi.org/10.1130/0091-7613(1979)7<104:MOAIMB>2.0.CO;2.

Masselink, G., Beetham, E. and Kench, P.D. (2020). Coral reef islands can accrete vertically in response to sea-level rise. *Science Advances.*

Masselink, G., Tuck, M., McCall, R., van Dongeren, A., Ford, M. and Kench, P.S. (2018), Physical and numerical modelling of infragravity wave generation and transformation on coral reef platforms. *Journal of Geophysical Research (Oceans)*, *124*, 1410–1433, https://doi.org/10.1029/2018JC014411.

Matias, A., Masselink, G., Castelle, B., Blenkinsopp, C. and Kroon, K. (2016) Measurements of morphodynamic and hydrodynamic overwash processes in a large-scale wave flume. *Coastal Engineering*, *113*, 33-46. http://dx.doi.org/10.1016/j.coastaleng.2015.08.005.

Mattias, A., Williams, J., Ferreira, O. and Masselink, G. (2012) Barrier overwash. *Coastal Engineering*, *63*, 48-61. http://dx.doi.org/10.1016/j.coastaleng.2011.12.006.

McCall, R.T., Masselink, G., Poate, T.G., Roelvink, J.A. and Almeida, L.P., 2015. Modelling the morphodynamics of gravel beaches during storms with XBeach-G, *Coastal Engineering*, *103*, 52–66, http://dx.doi.org/10.1016/j.coastaleng.2015.06.002.

McCall, R.T., Poate, T.G., Masselink, G. Roelvink, J.A., Almeida, L.P., Davidson, M. and Russell, P.E. (2014), Modelling storm hydrodynamics on gravel beaches with XBeach-G, *Coastal Engineering*, *91*, 231–250, http://dx.doi.org/10.1016/j.coastaleng.2014.06.007.

McCall, R.T., Van Thiel de Vries, J.S.M., Plant, N.G., Van Dongeren, A.R., Roelvink, J.A., Thompson, D.M. and Reniers A.J.H.M. (2010) Two-dimensional time dependent hurricane overwash and erosion modeling at Santa Rosa Island. *Coastal Engineering*, *57*, 668-683, https://doi.org/10.1016/j.coastaleng.2010.02.006.

Nielsen, P. (2002), Shear stress and sediment transport calculations for swash zone modelling. *Coastal Engineering*, *45*, 53–60, https://doi.org/10.1016/S0378-3839(01)00036-9.

Orford, J.D., Carter, R.W., Jennings, S.C. and Hinton, A.C. (1995), Processes and timescales by which a coastal gravel-dominated barrier responds geomorphologically to sea-level rise: Story head barrier, Nova Scotia. *Earth Surface Processes and Landforms*, *20*, 21–37, https://doi.org/10.1002/esp.3290200104.

Pandolfi, J.M., Connolly, S.R., Marshall, D.J. and Cohen, A.L (2011), Projecting coral reef futures under global warming and ocean acidification, *Science*, *333*, 418–422, https://doi.org/10.1126/science.1204794.

Pearson, S.G., Storlazzi, C.D., van Dongeren, A.R., Tissier, M.F.S. and Reniers, A.J.H.M. (2017), A Bayesian based system to assess wave-driven flooding hazards on coral reef-lined coasts, *Journal of Geophysical Research (Oceans), 122*, 10099–10117, https://doi.org/10.1002/2017JC013204.

Perry, C.T. et al. (2018), Loss of coral reef growth capacity to track future increases in sea level, *Nature*, *558*, 396–400. https://doi.org/10.1038/s41586-018-0194-z.

Perry, C.T., Edinger, E.N., Kench, P.S., Murphy, G.N., Smithers, S.G., Steneck, R.S. and Mumby, P.J. (2012), Estimating rates of biologically driven coral reef framework production and erosion: a new census-based carbonate budget methodology and applications to the reefs of Bonaire, *Coral Reefs*, *31*, 853–868, https://doi.org/10.1007/s00338-012-0901-4.

Perry, C.T., Kench, P.S., Smithers, S.G., Riegl, B., Yamano, H. and O'Leary, M.J. (2011) Implications of reef ecosystem change for the stability and maintenance of coral reef islands. *Global Change Biology*, *17*, 3679–3696, https://doi.org/10.1111/j.1365-2486.2011.02523.x.

Poate, T., Masselink, G., Austin, M.J., Dickson, M. and McCall, R. (2018), The role of bed roughness in wave transformation across rocky shore platforms, *Journal of Geophysical Research (Earth Surface)*, *123*, https://doi.org/10.1002/2017JF004277.

Quataert, E., Storlazzi, C.D., van Rooijen, A., Cheriton O. and van Dongeren, A. (2015), The influence of coral reefs and climate change on wave-driven flooding of tropical coastlines, *Geophysical Research Letters*, *42*, 6407-6415, https://doi.org/10.1002/2015GL064861.

Roelvink, J.A., Reniers, A., van Dongeren, A.R., van Thiel de Vries, J.S.M., McCall, R. and Lescinski, J. (2009), Modeling storm impacts on beaches, dunes and barrier islands, *Coastal Engineering*, *56*, 1133–1152, https://doi.org/10.1016/j.coastaleng.2009.08.006.

Ryan, E.J., Hamner, K. and Kench, P.S. (2019), Massive corals maintain positive carbonate budget of a Maldivian upper reef platform despite major bleaching event. *Scientific Reports, 6515*, https://doi.org/10.1038/s41598-019-42985-2.

Saunders, M., Albert, S., Roelfsema, C., Leon, J., Woodroffe, C., Phinn, S. and Mumby, P. (2016), Tectonic subsidence provides insight into possible coral reef futures under rapid sea-level rise, *Coral Reefs*, *35*, 155–167, https://doi.org/10.1007/s00338-015-1365-0.

Scoffin, T.P. (1993), The geological effects of hurricanes on coral reefs and the interpretation of storm deposits, *Coral Reefs*, *12*, 203–221, https://doi.org/10.1007/BF00334480.

Scopélitis, J., Andréfouët, S. Phinn, S., Done, T. and Chabanet, P. (2011), Coral colonisation of a shallow reef flat in response to rising sea level: quantification from 35 years of remote sensing data at Heron Island, Australia, *Coral Reefs*, *30*, 951, https://doi.org/10.1007/s00338-011-0774-y.

Smit, P., Stelling, G., Roelvink, J., Van Thiel de Vries, J., McCall, R., Van Dongeren, A., Zwinkels, C., Jacobs, R. (2010) *XBeach: Non-hydrostatic model: Validation, verification and model description*. Technical report, Delft University of Technology.

Stockdon, H.F., Holman, R.A., Howd, P.A., Howd, P.A. and Sallenger, A.H. (2006), Empirical parameterization of setup, swash, and runup, *Coastal Engineering*, *53*, 573-588, https://doi.org/10.1016/j.coastaleng.2005.12.005.

Stoddart D.R. and Steers J.A. (1977) The nature and origin of coral reef islands. In: *Biology and Geology of Coral Reefs*, Vol. IV, (eds Jones OA, Endean R), pp. 59–105. Academic Press, New York.

Storlazzi, C.D. et al. (2018), Most atolls will be uninhabitable by the mid-21st century because of sea-level rise exacerbating wave-driven flooding, *Science Advances*, *4*, eaap9741, https://doi.org/10.1126/sciadv.aap9741.

Storlazzi, C.D., Elias, E., Field, M.E. and Presto, M.K. (2011) Numerical modeling of the impact of sea-level rise on fringing coral reef hydrodynamics and sediment transport. *Coral Reefs*, 30, 83–96, https://doi.org/10.1007/s00338-011-0723-9.

Tuck, M., Ford, M.R., Masselink, G. and Kench, P.S. (2019a), Physical modelling of reef island topographic response to rising sea levels, *Geomorphology*, *345*, 106833, https://doi.org/10.1016/j.geomorph.2019.106833.

Tuck, M., Kench, P.S., Ford, M.R. and Masselink, G. (2019b), Physical modelling of the response of reef islands to sea level rise. *Geology*, *47*, 803–806, https://doi.org/10.1130/G46362.1.

Van Woesik, R. and Cacciapaglia, C.W. (2018), Keeping up with sea-level rise: Carbonate production rates in Palau and Yap, western Pacific Ocean, *PLoS One, 13(5)*, e0197077, https://doi.org/10.1371/journal.pone.0197077.

Van Woesik, R. and Cacciapaglia, C.W. (2019), Carbonate production of Micronesian reefs suppressed by thermal anomalies and Ancasthaster as sea-level rises, *PLoS One, 14(11)*, e0224887, https://doi.org/10.1371/journal.pone.0224887.

van Woesik, R., Golbuu, Y. and Roff, G. (2015), Keep up or drown: adjustment of western Pacific coral reefs to sea-level rise in the 21st century, *Royal Society Open Science*, 2, https://doi.org/10.1098/rsos.150181.

Wadey, M., Brown, S., Nicholls, R. and Haigh, I. (2017), Coastal flooding in the Maldives: an assessment of historic events and their implications, *Natural Hazards*, *89*, 131–159, https://doi.org/10.1007/s11069-017-2957-5.

Winter, G., et al. (2020) Steps to Develop Early Warning systems and future scenarios of storm wave-driven flooding along coral reef-lined coasts. *Frontiers in Marine Science*, *31*, https://doi.org/10.3389/fmars.2020.00199.

Woodroffe, C.D. (2008) Reef-island topography and the vulnerability of atolls to sea-level rise. *Global Planetary Change*, *62*, 77–96, https://doi.org/10.1016/j.gloplacha.2007.11.001.

Woodroffe, C.D. and Webster, J.M. (2014), Coral reefs and sea-level change, *Marine Geology*, *352*, 248–267, https://doi.org/10.1016/j.margeo.2013.12.006.

Yates, K.K., Zawada, D.G., Smiley, N.A. and Tiling-Range, G. (2017) Divergence of seafloor elevation and sea level rise in coral reef ecosystems. *Biogeosciences*, *14*, 1739–1772, https://doi.org/10.5194/bg-14-1739-2017.

Zijlema, M., Stelling, G. and Smit, P. (2011), Swash: an operational public domain code for simulating wave fields and rapidly varied flows in coastal waters. *Coastal Engineering*, *58*, 992–1012, https://doi.org/10.1016/j.coastaleng.2011.05.015.

719 **Supplementary Material 1 – BEWARE data set**
720
721

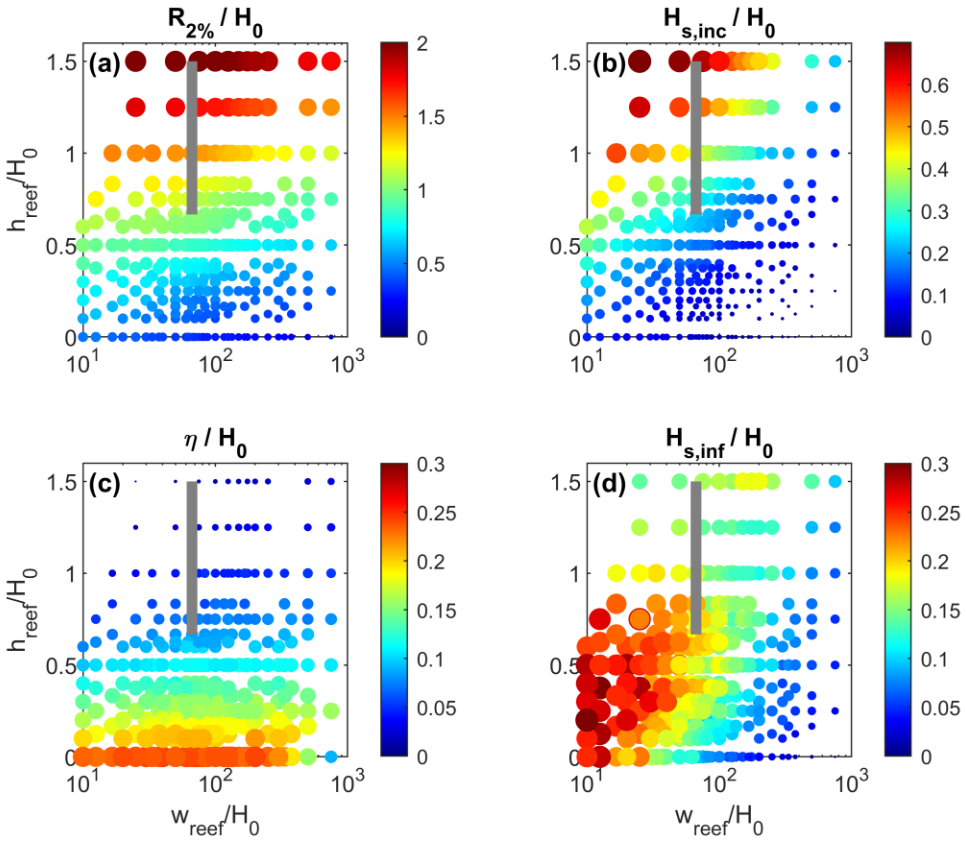

Figure **S1** – Scatter plots based on the BEWARE data set (Pearson et al., 2017) showing values of (a) runup $R_{2\%}$, (b) incident wave height $H_{s,inc}$, (c) wave setup η and (d) infragravity wave height $H_{s,inf}$, as a function of width of reef platform w_{reef} and still water depth over the reef platform h_{reef}. All parameters are normalized by the significant deep-water wave height H_0. Both bubble size and colour are proportional to the value of the parameter shown in the title of the subplots. Only a subset of the BEWARE data set is plotted, with the following parameters fixed: wave steepness H_0/L_0 = 0.025 (and peak wave period T_p = 6–20 s), fore reef slope $\tan\beta_{reef}$ = 0.1, bed roughness c_f = 0.05, beach slope $\tan\beta_{beach}$ = 0.1. The following parameters are variable in the data set: h_{reef} (0, 0.5, 1.0, 1.5, 2.0, 2.5, 3.0 m), H_0 (1, 2, 3, 4, 5 m) and w_{reef} (0, 50, 100, 150, 200, 250, 300, 350, 400, 500, 1000, 1500 m). The thick grey line represents the range of conditions modelled in the present paper (H_0 = 3 m, h_{reef} is 2–4.5 m and w_{reef} = 200 m; thus, h_{reef}/H_0 = 0.67–1.5 and w_{reef}/H_0 = 67). [p_beware_axes]

722
723

Supplementary Material 2 – XBeach-G model animations

Movies **S1** – Response of a gravel island to a 2.5-m sea-level rise. Because the gravel is very permeable, waves that overwash the island very quickly seep into the gravel. This results in island retreat and the deposition of gravel very close to the ocean edge in the form of a narrow and high ridge.

Movies **S2** – Response of a sand island to a 2.5-m sea-level rise. Because the sand is not very permeable, waves that overwash the island flow all the way to the back of the island, into the lagoon. This results in island retreat and the deposition of sand across the whole island, including into the lagoon, in the form of washovers.

Movies **S3** – With a relatively modest storm wave height of 2 m only a small number of waves overwash the island and the average overwash discharge tends to be less than 20 liters per meter per second. This will result in sediment deposition around the crest and across the back of the island, enabling the island to keep up with rising sea level'

Movies **S4** – With an extreme storm wave height of 4 m almost all waves overwash the island and even continue to travel into the lagoon. The average overwash discharge can be more than 100 liters per meter per second. This will result in removal of sediment from the entire island and will ultimately lead to the destruction and drowning of the island.